Wavelet analysis of intermittent momentum flux in the inertial subrange

U. GIOSTRA [1], S. SCHIPA [1] and D. CAVA [1][2]
[1] *ISIAtA/CNR - Lecce, Italy*
[2] *Dipartimento Scienza dei Materiali - Lecce, Italy*

(ricevuto il 22 Febbraio 1999; revisionato il 15 Ottobre 1999; approvato il 3 Febbraio 2000)

Summary. — In order to study the structure of the momentum flux in the inertial subrange, wavelet transforms have been performed on wind velocity time series. A conditional sampling has been utilised for separating intermittent contributions. A quadrant analysis technique has been applied to the intermittent and non-intermittent momentum fluxes. Their dependence on length scales, quadrants and stability has been investigated.

PACS 92.60.Fm – Boundary layer structure and processes.
PACS 47.27.Qb – Turbulent diffusion.
PACS 02.30.Qy – Integral transforms and operational calculus.

Symbols

$\mathrm{d}y$	= *measurement spacing in physical space*
$\mathrm{D}u$	= *longitudinal velocity difference*
$f(t)$	= *real square integrable function*
H	= *hole size*
$I(m)$	= *intermittence indicator function*
k	= *position index*
K_n	= *universal constants for structure function of order n*
L	= *Monin-Obukhov length*
m	= *scale index*
n	= *order of the structure function*
$N(m)$	= *number of wavelet coefficients at scale m*
q	= *quadrant index*
r	= *separation distance*
$S_{q,H}$	= *momentum flux fraction*
t	= *position translation*
$T_{q,H}$	= *time fraction*
u, v, w	= *velocity components*
U	= *mean longitudinal velocity*

$u_{(\mathrm{int})}\%$ = *percentage of intermittent events in the longitudinal wind component*
$uw(m)$ = *mean momentum flux*
$uw_{(\mathrm{int})}(m)$ = *intermittent momentum flux*
$uw_{(\mathrm{con})}(m)$ = *conditioned momentum flux*
x, y, z = *spatial coordinates*
$w_{(\mathrm{int})}\%$ = *percentage of intermittent events in the vertical wind component*
ε = *turbulent kinetic energy dissipation*
ζ = *z/L stability parameter*
λ = *scale dilation*
ν = *kinematic viscosity*
$\psi_{\lambda, t}(\tau)$ = *wavelet functions*
$\Delta f(\lambda, t)$ = *wavelet transform*
$\langle\,\rangle$ = *time average operator*
$\langle\,\rangle_{(\mathrm{con})}$ = *conditioned time average operator*

1. – Introduction

The dissipation of turbulent kinetic energy ε plays a fundamental role in the local structure of turbulence [1]. This role is elucidated by the Kolmogorov similarity hypotheses [2], from which the well-known structure functions result:

$$\langle |\mathrm{D}u|^n \rangle = K_n (\langle \varepsilon \rangle)^{n/3} r^{n/3}, \tag{1}$$

where n is the structure function order, $\mathrm{D}u$ is the longitudinal velocity difference between two points separated by a distance r, K_n are universal constants and $\langle\,\rangle$ is a time average operator over a statistically stationary flow.

However, in a small fraction of the fluid volume large dissipation of turbulent kinetic energy can occur, so that ε exhibits an intermittent behaviour and its average value is not significative enough for describing the local nature of the similarity hypotheses [3]. The effect of fluctuations in energy dissipation rate on the small-scale properties of turbulence determines a deviation from relationships (1). This deviation has been related (first by Landau, see [1], p. 584; [4], p. 126) to the inequality between $\langle \varepsilon \rangle^n$ and $\langle \varepsilon^n \rangle$, so that the departure is more evident for large values of n (see, *e.g.*, [5], for an extensive discussion).

If the events responsible for the breakdown of the Kolmogorov similarity hypotheses can be detected, a conditional sampling on intermittent events can be performed. It is well known that extreme events largely contribute to turbulent fluxes. The aim of this paper is to compare the structure of intermittent and not intermittent components of the turbulent fluxes, and their dependence on stability, if any.

Following Katul *et al.* [6], hereinafter KACP, conditional wavelet statistics able to identify the location of large dissipation events in the inertial subrange have been used. This conditional sampling has been applied to several wind velocity data set measured in an atmospheric surface layer, with thermal stratification ranging from neutral to moderately stable ($0 < \zeta < 1$, where $\zeta = z/L$ and L is the Monin-Obukhov length). Then, in order to investigate the dependence of the conditioned data set on the hole size, *i.e.* on the intensity of momentum transport, a quadrant technique [7] has been carried out. Flux and time fraction diagrams enlighten the different behaviour between intermittent and non-intermittent momentum fluxes. These differences are function of the stability, of the length scale, and, overall, of the quadrants.

A brief description of measurement site and data analysis is given in sect. **2**. Basic information on the wavelet transforms and on the conditional sampling used is presented in sect. **3**. The quadrant analysis technique, both for flux and time fractions, is described in sect. **4**. Finally, a discussion of the results is summarised in sect. **5**.

2. – Measurement site and data analysis

The turbulent data here analysed have been sampled throughout the period from November 20th, 1993 to February 12th, 1994, on the Nancen Ice Sheet, a permanently frozen branch of the Ross Sea, Antarctica. More information about site characteristics can be found in Giostra *et al.* [8] and Cava *et al.* [9].

The micrometeorological tower was located at 74° 41′ 58″ S and 163° 30′ 50″ E, in the middle of a homogeneous snowy area of $50 \times 3\ \mathrm{km}^2$, gently sloping ($\approx 0.4\%$) along the north-south axis.

Turbulence measurements have been performed at three levels (2, 4.5, and 10 meters) by symmetric 3-axis ultrasonic anemometers (Gill Inst. Ltd.). Wind velocity components and sonic temperature have been sampled at a frequency of 20.8 Hz.

To avoid errors due to misalignment of ultrasonic anemometers with local streamlines, data have been rotated [10] in a "streamline system".

3. – Wavelet transforms

Wavelet transforms are mathematical techniques that can unfold signals in components of different frequencies, allowing resolutions matched to any scale (see, *e.g.*, [11]).

Wavelet transforms are based on group theory and square-integrable representation; they are transforms localised both in time (or space, using the frozen turbulence hypothesis) and in frequency; they can be classified either as continuous or as discrete. The continuous wavelet transform of a real square integrable function $f(t)$ can be defined as

$$\Delta f(\lambda, t) = \int_{-\infty}^{+\infty} f(\tau)\, \frac{1}{\sqrt{\lambda}}\, \psi\left(\frac{\tau - t}{\lambda}\right) \mathrm{d}\tau\,, \tag{2}$$

$\psi_{\lambda, t}(\tau) \equiv (1/\sqrt{\lambda})\, \psi((\tau - t)/\lambda)$ are the wavelet functions obtained by dilating the *mother wavelet* $\psi(t)$ of an amount λ (scale dilation) and by shifting $\psi(t)$ in time of the quantity t (position translation).

Discrete wavelet transforms can be obtained by discretizating λ and t:

$$\Delta f(m, k) = \lambda_0^{-m/2} \int f(t)\, \psi(\lambda_0^{-m} t - k t_0)\, \mathrm{d}t\,, \tag{3}$$

where $\lambda_0 > 1$ is the base of dilation and m is the corresponding integer scale index; $t_0 > 0$ is the translation length and k is the corresponding integer scale index. Then, $\lambda = \lambda_0^m$ and $t = k t_0 \lambda_0^m$.

For turbulence measurements orthonormal discrete wavelet transforms are preferred, both because they form a complete basis with mutually orthogonal kernel functions, and because they give a physical interpretation of the expansion coefficients from the energetic point of view. In particular, choosing $\lambda_0 = 2$ and $t_0 = 1$, a complete

orthonormal basis $(\psi_{m,k}(t))$ for all functions having finite energy can be created:

$$\psi_{m,k}(t) = 2^{-m/2}\psi(2^{-m}t - k). \tag{4}$$

In this way, $f(t)$ can be approximated, up to arbitrary high precision, by a linear combination of the wavelets $\psi_{m,k}(t)$, *i.e.*

$$f(t) = \sum_m \sum_k \Delta f(m, k)\, \psi_{m,k}(t). \tag{5}$$

Therefore, the wavelets provide a time-scale representation of the process where time and scale locations are given by indices k and m, respectively [12].

The Haar wavelet is frequently used in geophysics applications, giving an excellent localisation in physical space. Moreover, the differencing characteristics of the Haar wavelet allow explicit relations between the n-th order structure function and the wavelet coefficients.

The Haar function defined as follows:

$$\Psi(x) = \begin{cases} +1\,, & -0.5 \leqslant x \leqslant 0\,, \\ -1\,, & 0 < x \leqslant +0.5\,, \\ 0\,, & \text{otherwise} \end{cases} \tag{6}$$

constitutes an orthonormal basis for all functions that have finite energy.

In this work, the Haar wavelet is applied to wind velocity components:

$$u_i,\ v_i,\ w_i \qquad \text{with } i = 1,\ 2^M,$$

where $M = 16$ and $2^M = 65536$ data points.

Difference terms, corresponding to Haar transform values, describe variations in the wind component; for the longitudinal component, they are defined as

$$\Delta u(m, k) = \frac{1}{2^m} \sum_{j=1}^{2^{m-1}} (u_{2^m(k-1/2)+j} - u_{2^m(k-1)+j}) \tag{7}$$

and they characterise the average change in the u signal on the scale m across the interval $[2^m(k-1),\ 2^m k]$, with $k = 1,\ 2^{M-m}$ [13].

Such wavelet coefficients can be related [6, 13], to the n-th order function:

$$\langle |u(x+r) - u(x)|^n \rangle \sim \frac{\langle |\Delta u(m, k)|^n \rangle}{(\mathrm{d}y)^n}\,, \tag{8}$$

where $r = 2^m\,\mathrm{d}y$ is the separation distance (in meters); $\mathrm{d}y = f_s^{-1} U$, f_s is the sampling frequency and U is the mean longitudinal velocity; $\langle\,\rangle$, on the right side of (8), is the averaging operator applied to the wavelet coefficients over all values of the position index k at scale m. As already mentioned, the structure functions diverge from theoretical relationships (see eq. (1)) because of the intermittency.

The intermittency results in intense and isolated dissipation events. These events interest only small fluid fractions, surrounded by passive fluid. In Tennekes and

Lumley [14] the turbulent kinetic energy dissipation rate in isotropic turbulence is

$$\langle \varepsilon \rangle = 15 \nu \left\langle \left[\frac{\partial u}{\partial x} \right]^2 \right\rangle, \tag{9}$$

where ν is the kinematic viscosity and u the velocity fluctuation in the longitudinal direction. Moreover, Tennekes [15] suggested that intermittency results in a large spatial variance in the dissipation σ_ε^2 around its mean value $\langle \varepsilon \rangle$. Using these arguments, KACP have proposed a relation between ε and the wavelet coefficients (see [6], eq. (22)). A threshold value equal to 5 times the averaged squared wavelet coefficients at scale index m is proposed by KACP to select intermittent events:

$$[\Delta u(m, k)]^2 > 5 \langle [\Delta u(m, k)]^2 \rangle . \tag{10}$$

Applying this conditioning criterion, the data set can be splitted into an intermittent and a non-intermittent subset. Therefore, a conditional n-th order structure function can be defined as

$$\langle |u(x + r) - u(x)|^n \rangle_{(\mathrm{con})} \sim \frac{\langle\!\langle |I(m)\, \Delta u(m, k)|^n \rangle\!\rangle}{(\mathrm{d}y)^n} , \tag{11}$$

where hereinafter the subscript (con) refers to conditioned quantities; $I(m)$ is the intermittence indicator function at scale m, which is equal to 0 or 1, depending on whether (10) is satisfied or not. $\langle\!\langle\ \rangle\!\rangle$ is the averaging operator over all non-zero values of $[I(m)\, \Delta u(m, k)]$.

4. – Quadrant analysis

Intermittency in the atmospheric boundary layer can account for a large portion of flux transport of scalars such as momentum and heat. The role of intermittent events can be investigated using the quadrant analysis technique [7].

This method sorts the momentum transport into quadrants according to the signs of $\Delta u(m, k)$ and $\Delta w(m, k)$, *i.e.* to the longitudinal and vertical wind components wavelet coefficients.

The four quadrants ($q = 1, 2, 3, 4$) in which the momentum flux is partitioned are defined in the following way:

$q = 1$ when $\Delta u(m, k) > 0$ and $\Delta w(m, k) > 0$, outward interaction or reflection;
$q = 2$ when $\Delta u(m, k) < 0$ and $\Delta w(m, k) > 0$, ejection;
$q = 3$ when $\Delta u(m, k) < 0$ and $\Delta w(m, k) < 0$, inward interaction or deflection;
$q = 4$ when $\Delta u(m, k) > 0$ and $\Delta w(m, k) < 0$, sweep.

"Ejections" are produced by slow air moving from the surface, whereas "sweeps" are produced by fast air moving down. Both these structures give a negative momentum flux. On the other hand, reflections and deflections represent the interactions between ejections and sweeps, giving a positive contribution to the momentum transport [16].

The intensity of contributions to the intermittent and non-intermittent fluxes can be analysed as a function of total momentum flux. Therefore, a threshold parameter H, called hole size, is introduced.

On the scale m, the conditional average of the vertical momentum flux $\langle \Delta u(m, k)^* \Delta w(m, k) \rangle_{q, H}$, in the q-th quadrant and outside of a hole size H, is the following:

$$\langle \Delta u(m, k)^* \Delta w(m, k) \rangle_{q, H} = \frac{1}{N(m)} \sum_k (\Delta u(m, k)^* \Delta w(m, k)) I_{q, H, k}, \tag{12}$$

where $N(m)$ is the number of wavelet coefficients of scale m; $I_{q, H, k}$ is an indicator function defined as

$$I_{q, H, k} = \begin{cases} 1 \text{ when the point } (\Delta u(m, k), \Delta w(m, k)) \text{ is in quadrant } q \text{ and} \\ |\Delta u(m, k)^* \Delta w(m, k)| > H \left| \sum_m uw(m) \right|, \\ 0 \text{ otherwise (the point is inside the hole)}, \end{cases} \tag{13}$$

$$uw(m) = \frac{1}{2^{M-m}} \sum_k (\Delta u^{(m)}(k)^* \Delta w^{(m)}(k)) \tag{14}$$

is the mean momentum flux of the scale m, and $\sum_m uw(m)$ the total of the mean flux of every scale.

Therefore, the threshold H selects the flux contribution H times greater than the total momentum flux.

The conditionally averaged momentum flux is then defined as

$$S_{q, H} = \langle \Delta u(m, k)^* \Delta w(m, k) \rangle_{q, H} \Big/ \left| \sum_m uw(m) \right|. \tag{15}$$

Moreover, analogously to the flux fraction (eq. (15)), it is possible to calculate the time fraction as follows:

$$T_{q, H} = \frac{1}{N(m)} \sum_k I_{q, H, k}. \tag{16}$$

The described quadrant analysis can be applied both to the intermittent and non-intermittent subset, in order to investigate their structure on different scale m, their dependence on stability and their intensity (*i.e.* their dependence on H).

5. – Results and discussion

As a first step, we have applied the conditional sampling (eq. (10)) to the data set. As expected (see, for example, [17]), the effects of intermittency are enhanced for large values of the structure function order n. The analysis of the sixth-order structure function corroborates the reliability of the wavelet conditional sampling.

Figure 1 shows the suppression of intermittence in the conditioned structure functions. Two cases with different thermal stratification are presented. Since the inertial subrange is not affected by stability, no significant differences are expected. Both the regression fits approach the theoretical slope.

If the KACP conditional sampling has efficiently suppressed the intermittency, the velocity statistics within the inertial subrange do not differ significantly from a

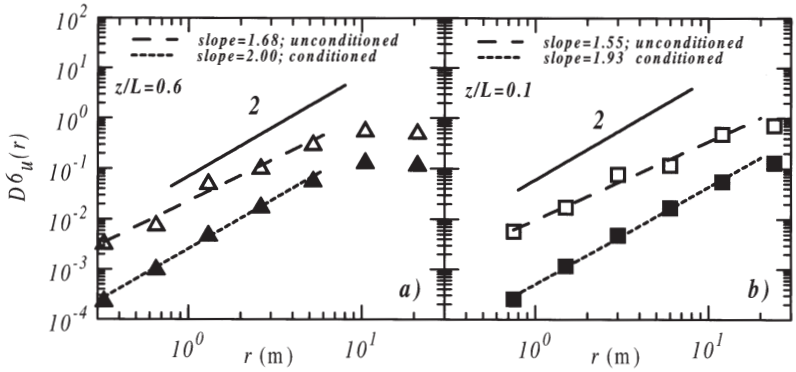

Fig. 1. – Comparison between conditioned and unconditioned sixth-order wavelet structure functions, relative to: a) data sampled in the period 00–01 a.m. of January 30th 1994, $U = 3.4$ m/s and $z/L = 0.6$; b) data sampled in the period 10–11 a.m. of January 23rd 1993, $U = 7.8$ m/s and $z/L = 0.1$. Continuous lines represent the theoretical slope in the inertial subrange; dashed and dotted lines represent regression fits of unconditioned and conditioned data, respectively.

Gaussian [18]. In fig. 2a) the probability density function (pdf) of the three velocity components for the scale $m = 4$ (corresponding to 1.3 Hz or, using the frozen turbulence hypothesis, $r = 6$ m) is shown. The effect of the conditional sampling is evident in fig. 2b), where all the velocity component pdfs approach a Gaussian. Noteworthy, standard deviation values are quite similar ($\sigma_u = 0.13$ m/s, $\sigma_v = 0.14$ m/s, $\sigma_w = 0.12$ m/s), reflecting the isotropy of the inertial subrange.

The skewness (Sk) and kurtosis (Ku) as a function of separation distance r are shown in fig. 3, both for conditioned and unconditioned cases. A Gaussian statistic (*i.e.*, $Sk = 0$ and $Ku = 3$) is approached in the whole inertial subrange.

The conditional sampling has been applied to data set with stability ranging from neutral to moderately stable conditions ($0 < \zeta < 1$). The proposed tests (Gaussian behaviour of the velocity statistics and structure function slopes) have shown that the intermittence is suppressed irrespectively to stability. Therefore, the contributions of

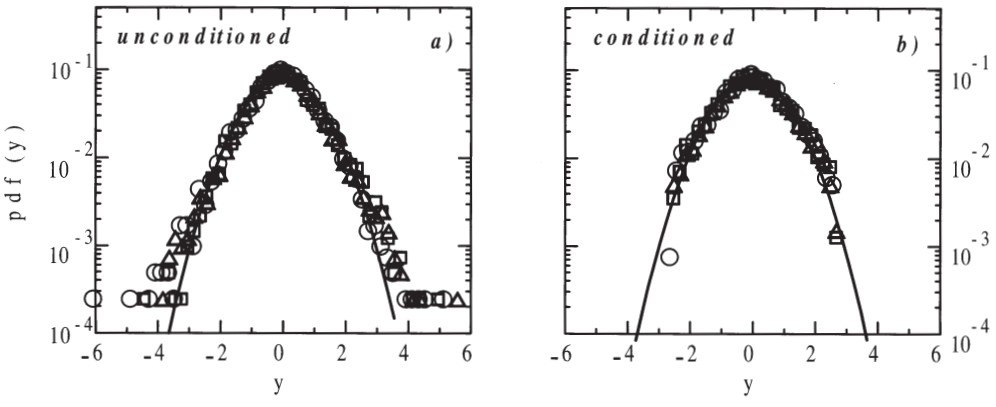

Fig. 2. – Probability density functions for a) unconditioned and b) conditioned data of the three velocity components for the scale $m = 4$; data are relative to the same period shown in fig. 1b).

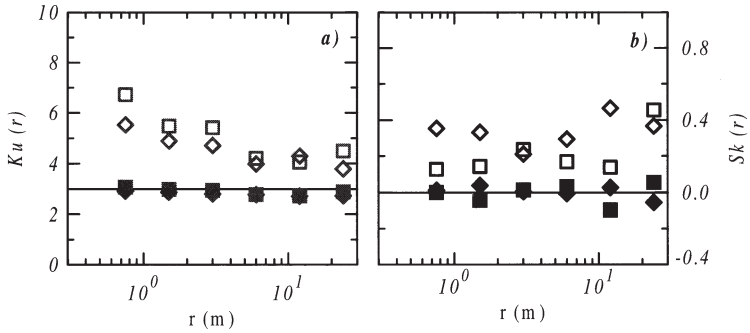

Fig. 3. – Kurtosis (a) and skewness (b) of longitudinal (diamonds) and vertical (squares) probability density functions relative to the data set shown in fig. 1b). Empty symbols refer to unconditioned data, full symbols to conditioned ones.

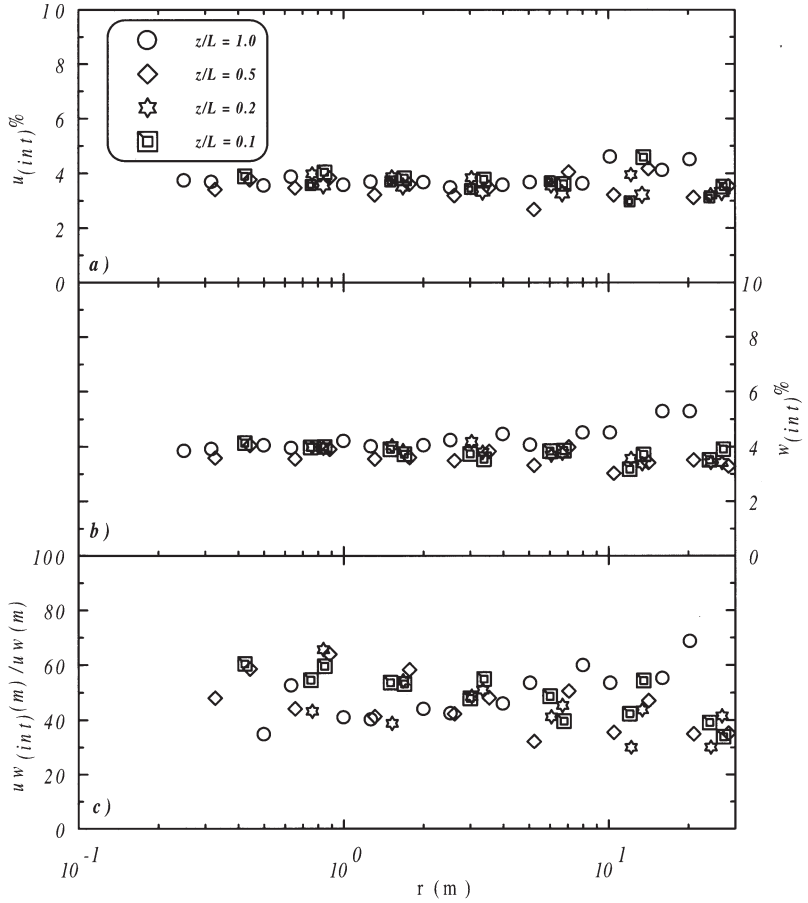

Fig. 4. – Percentage of intermittent events $u_{(\mathrm{int})}\%$ in the longitudinal wind component (a), $w_{(\mathrm{int})}\%$ in the vertical one (b), and percentage of intermittent momentum flux (c) as a function of separation distance r and for different atmospheric stability conditions.

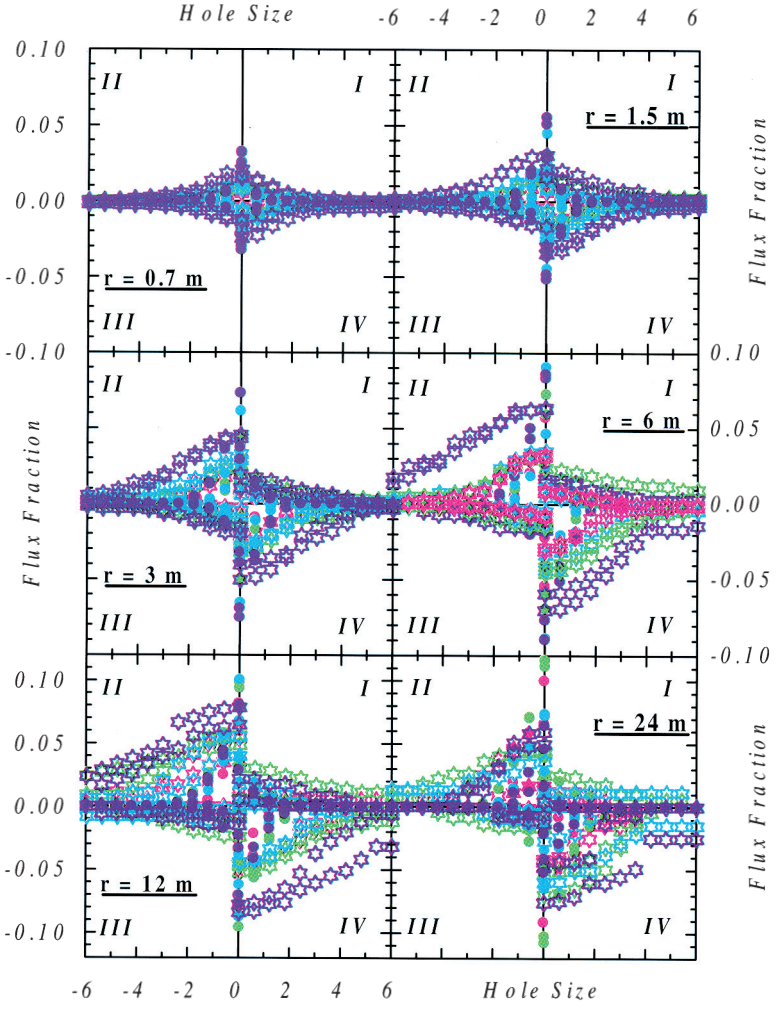

Fig. 5. – Quadrant representation of the intermittent (empty stars) and non-intermittent (full points) flux fraction at different scales r and for different atmospheric stability conditions. Symbol colours refer to: blue to $z/L \approx 1.0$; cyan to $z/L \approx 0.5$; green to $z/L \approx 0.2$ and magenta to $z/L \approx 0.1$.

both the conditioned (Gaussian) and intermittent parts of the flow can be separately investigated.

First of all, it can be observed that only a small fraction ($\cong 4\%$) of the velocity fluctuations (*i.e.* of the wavelet coefficients) is intermittent, both for longitudinal and vertical components (see figs. 4a), b)). Note that this fraction depends neither on the length scale, nor on the stability in the whole inertial subrange. We split the mean momentum flux, defined in eq. (14), into an intermittent $uw_{(\mathrm{int})}(m)$ and in a conditioned $uw_{(\mathrm{con})}(m)$ contribution (where $uw_{(\mathrm{con})}(m) = uw(m) - uw_{(\mathrm{int})}(m)$). We define the intermittent momentum flux at scale m, as the cross-correlation between $\Delta u(m, k)$ and $\Delta w(m, k)$ when at least one velocity component is intermittent. Despite its moderate occurrence, the intermittent momentum flux $uw_{(\mathrm{int})}(m)$ contributes to the total

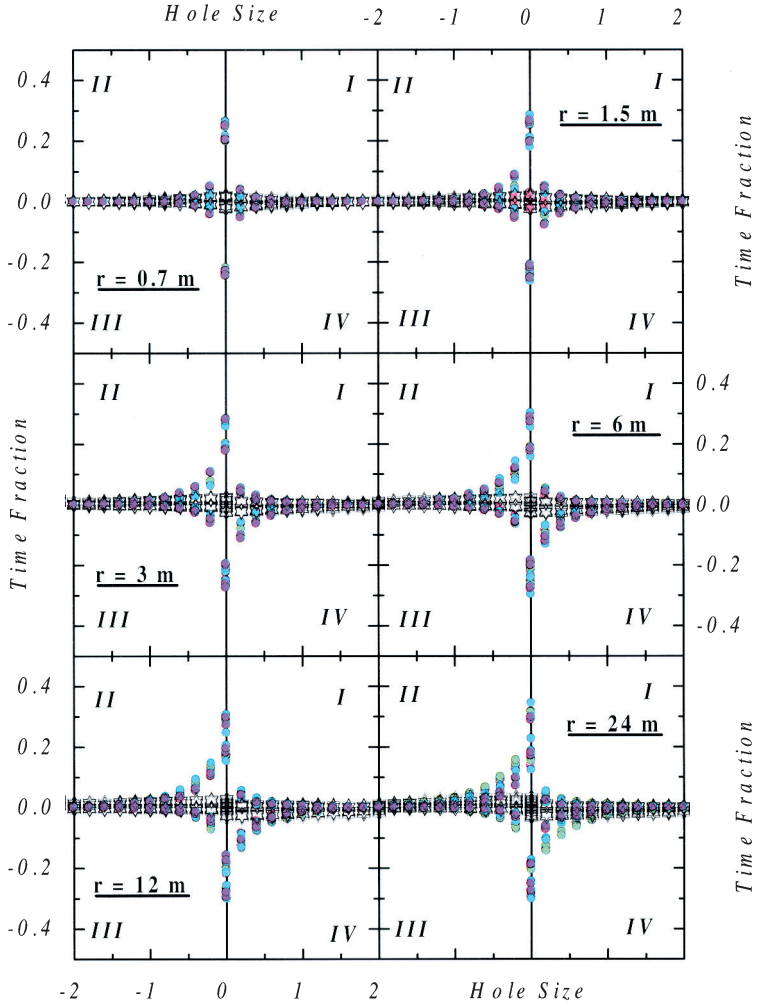

Fig. 6. – As in fig. 5, but for time fraction.

momentum flux $uw(m)$ as efficiently as the conditioned momentum flux $uw_{(\mathrm{con})}(m)$ (see fig. 4c)). Again, the independence on the length scale and on the stability is remarkable.

Using the above-presented quadrant analysis, a comparison between $uw_{(\mathrm{int})}(m)$ and $uw_{(\mathrm{con})}(m)$ as a function of quadrants, length scale and stability has been performed.

Figure 5 summarises this comparison for the flux fraction. At small scale ($r<1.5$ m) the overall behaviour is similar for both the intermittent and the conditioned fluxes; *i.e.*, the flux fractions have the same intensity and sharply decrease as a function of the hole size in all four quadrants. Therefore, it should be pointed out that, at small scale, i) large intermittent fluctuations are inhibited, and ii) since the upward momentum transport is comparable with the downward one (see, *e.g.*, [7]), contributions to the total momentum flux are small. A weak dependence on stability is observed.

When the length scale increases, the contribution of ejections and sweeps (quadrants 2 and 4) becomes dominant with respect to reflections and deflections (quadrants 1 and 3), giving rise to a typical butterfly shape. Therefore, the total momentum flux (*i.e.* the difference between even and odd quadrants) becomes negative, driven by ejections and sweeps. The values of the intermittent and conditioned flux fractions are similar for a hole size $H = 0$, according to fig. 4c). However, $uw_{(\mathrm{int})}(m)$ and $uw_{(\mathrm{con})}(m)$ exhibit different behaviours as H increases, *i.e.* looking at even more energetic contributions. Specifically, $uw_{(\mathrm{int})}(m)$ is larger than $uw_{(\mathrm{con})}(m)$, thus reflecting the strong intensity of the instantaneous intermittent contributions to the total flux.

The clear dependence on stability is remarkable: although the total intermittent contribution to the total momentum flux (about 40%) does not depend on stability, the energy associated to the intermittent events does. At the largest scale here analysed ($r = 24$ m), the energetic intermittent contributions ($H \gg 1$) are weakened in the more stable cases ($\zeta \cong 1$). Odd quadrants seem less sensitive than even quadrants with respect to both hole size and stability.

More information can be obtained by the time fraction quadrant analysis (fig. 6). As expected, the $uw_{(\mathrm{int})}(m)$ time fraction is much smaller than the $uw_{(\mathrm{con})}(m)$ time fraction irrespectively of length scale, hole size, and stability. Therefore, the same momentum quantity ($uw_{(\mathrm{int})}(m) \cong uw_{(\mathrm{con})}(m)$) is transported by intermittent fluctuations more efficiently (typically 15 times more efficiently) than by the non-intermittent ones.

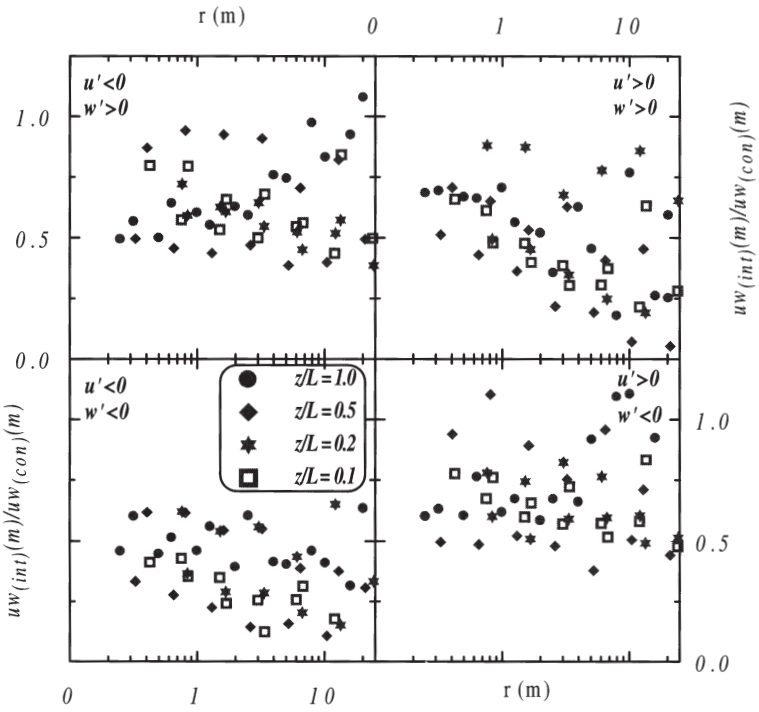

Fig. 7. – Ratio of intermittent and non-intermittent vertical momentum flux as a function of the distance separation r for all quadrants. Different symbols refer to different atmospheric stability conditions.

Conditioned flux exhibits an asymmetry between odd and even quadrants (more evident in the larger scales); *i.e.* energetic events are more persistent or frequent in ejections and sweeps.

Figure 7 enlightens the $uw_{(\mathrm{int})}(m)$ and $uw_{(\mathrm{con})}(m)$ dependence on length scale. Once again, even and odd quadrants show different behaviours. In the odd quadrants the ratio $uw_{(\mathrm{int})}(m)/uw_{(\mathrm{con})}(m)$ decreases as the length scale r increases, whereas in the even quadrants the ratio increases as r increases. Therefore, the role of intermittence is emphasised in ejections and sweeps.

6. – Conclusions

In order to detect intermittent events in the inertial subrange, a conditional sampling based on wavelet spectral analysis [6] has been performed on wind velocity data set. Data are referred to measurements collected in an atmospheric surface layer over a flat and homogeneous terrain. The thermal stratification ranged from neutral to moderately stable condition ($0 < \zeta < 1$). The reliability of the conditional sampling has been validated comparing the conditioned wavelet statistics to the theoretical structure functions and to the expected Gaussian statistics in the inertial subrange. A comparison between intermittent and non-intermittent momentum fluxes has been performed using a quadrant technique. Their dependence on length scale, quadrants and stability has been investigated.

To summarise, the following results can be enlightened: i) the intermittent and non-intermittent momentum flux intensities are quite similar in the inertial subrange; ii) intermittent events are active in a small time fraction ($\leqslant 10\%$); iii) neglecting the smaller scales ($r \leqslant 1$ m), ejections and sweeps are the most energetic mechanisms for the momentum transport both for intermittent and non-intermittent fluxes; iv) the intermittent fractional flux is still intense for large hole size, evidencing extremely intense events; v) quadrant analysis as a function of hole size detects a dependence on stability; the independence from stability of both the total intermittent and the total non-intermittent momentum flux is remarkable; vi) the ratio $uw_{(\mathrm{int})}(m)/uw_{(\mathrm{con})}(m)$ decreases in the odd quadrants as the length scale r increases; on the contrary $uw_{(\mathrm{int})}(m)/uw_{(\mathrm{con})}(m)$ increases in the even quadrants as r increases; therefore intermittence is enhanced in large ejections and sweeps occurrence.

* * *

This work has been partially developed in the frame of the CNR-PAT Project "Analisi teorica e sperimentale dei processi di scambio di energia e materia tra ecosistemi forestali e atmosfera", and partially in the frame of the Italian National Program for Research in Antarctica (PNRA).

REFERENCES

[1] MONIN A. S. and YAGLOM A. M., *Statistical Fluid Mechanics*, edited by J. LUMLEY, Vol. **II** (MIT Press) 1975.

[2] KOLMOGOROV A. N., *The local structure of turbulence in incompressible viscous fluid for very large Reynolds numbers*, *Dokl. Akad. Nauk SSSR*, **4** (1941) 299-303.

[3] NOVIKOV E. A., *Variation in the dissipation of energy in a turbulent flow and the spectral distribution of energy, Appl. Math. Mech.*, **27** (1963) 1445-1450.
[4] LANDAU L. D. and LIFSHITZ E. M., *Fluid Mechanics* (Pergamon Press) 1986.
[5] FRISCH U., *Turbulence, the Legacy of A. N. Kolmogorov* (Cambridge University Press, Cambridge) 1995.
[6] KATUL G. G., ALBERTSON J. D., CHU C. B. and PARLANGE M. B., *Intermittency in Atmospheric Surface Layer Turbulence: The Orthonormal Wavelet Representation*, in *Wavelets in Geophysics* (Academic Press, Inc.) 1994, pp. 81-105.
[7] HAYASHI T., *An analysis of wind velocity fluctuations in the atmospheric surface layer using an orthonormal wavelet transform, Boundary Layer Meteorol.*, **70** (1994) 307-326.
[8] GIOSTRA U., CAVA D., CARDILLO F. and TAGLIAZUCCA M., *Some characteristics of turbulence from summertime measurements over an Antarctic Ice Sheet, Conference Proceedings of the 6th Workshop - Italian Research on Antarctic Atmosphere*, edited by M. COLACINO, G. GIOVANELLI and L. STEFANUTTI, Vol. **51** (Editrice Compositori, Bologna) 1996, pp. 25-38.
[9] CAVA D., GIOSTRA U., TROMBETTI F. and TAGLIAZUCCA M., *Turbulence characteristics of a stable boundary layer over sloping terrain, Proceedings of the Fifth International Conference AIR POLLUTION 97, Bologna (Italy), 16-18 September*, edited by H. POWER, T. TIRABASSI and C. A. BREBBIA (1997), pp. 91-100.
[10] MCMILLEN R. T., *An eddy correlation technique with extended applicability to non-simple terrain, Boundary Layer Meteorol.*, **43** (1988) 231-245.
[11] FARGE M., *Wavelet transforms and their applications to turbulence, Ann. Rev. Fluid Mech.*, **24** (1992) 395-457.
[12] FOUFOULA-GEORGIOU E. and KUMAR P., *Wavelet analysis in geophysics: An introduction*, in *Wavelets in Geophysics* (Academic Press, Inc.) 1994, pp. 1-43.
[13] HOWELL J. F. and MAHRT L., *An adaptive decomposition: Application to turbulence*, in *Wavelets in Geophysics* (Academic Press, Inc.) 1994, pp. 107-128.
[14] TENNEKES H. and LUMLEY J. L., *A First Course in Turbulence* (MIT Press) 1990.
[15] TENNEKES H., *Intermittency of the small-scale structure of atmospheric turbulence, Boundary Layer Meteorol.*, **4** (1973) 241-250.
[16] LYKOSSOV V. N. and WAMSER C., *Turbulence Intermittency in the Atmospheric Surface Layer Over Snow-Covered Sites, Boundary Layer Meteorol.*, **72** (1995) 393-409.
[17] ANSELMET F., GAGNE Y., HOPFINGER E. J. and ANTONIA R. A., *High-order velocity structure functions in turbulent shear flows, J. Fluid Mech.*, **140** (1984) 63-89.
[18] KRAICHNAN R., *Turbulent cascade and intermittent growth, Turbulence and Stochastic Processes: Kolmogorov's Ideas 50 Years On*, edited by J. HUNT, M. PHILLIPS and D. WILLIAMS (Royal Society, London) 1991.